

Thermoelectric characteristics of flexible reduced graphene oxide/silver selenide nanowire composites prepared by a facile vacuum filtration process

Zuo Xiao(肖佐), Yong Du(杜永) , Qiufeng Meng(孟秋风) , and Lei Wang(王磊)

Citation: Chin. Phys. B, 2022, 31 (**2**): 028103. DOI: 10.1088/1674-1056/ac447e
Journal homepage: http://cpb.iphy.ac.cn; http://iopscience.iop.org/cpb

What follows is a list of articles you may be interested in

Enhancing the thermoelectric performance through the mutual interaction between conjugated polyelectrolytes and single-walled carbon nanotubes

Shuxun Wan(万树勋), Zhongming Chen(陈忠明), Liping Hao(郝丽苹), Shichao Wang(王世超), Benzhang Li(李本章), Xiao Li(黎潇), Chengjun Pan(潘成军), and Lei Wang(王雷)
Chin. Phys. B, 2022, 31 (**2**): 028104. DOI: 10.1088/1674-1056/ac48f9

Super deformability and thermoelectricity of bulk *γ*-InSe single crystals

Bin Zhang(张斌), Hong Wu(吴宏), Kunling Peng(彭坤岭), Xingchen Shen(沈星辰), Xiangnan Gong(公祥南), Sikang Zheng(郑思康), Xu Lu(卢旭), Guoyu Wang(王国玉), and Xiaoyuan Zhou(周小元)
Chin. Phys. B, 2021, 30 (**7**): 078101. DOI: 10.1088/1674-1056/abf133

Epitaxial synthesis and electronic properties of monolayer Pd_2Se_3

Peng Fan(范朋), Rui-Zi Zhang(张瑞梓), Jing Qi(戚竞), En Li(李恩), Guo-Jian Qian(钱国健), Hui Chen(陈辉), Dong-Fei Wang(王东飞), Qi Zheng(郑琦), Qin Wang(汪琴), Xiao Lin(林晓), Yu-Yang Zhang(张余洋), Shixuan Du(杜世萱), Hofer W A, Hong-Jun Gao(高鸿钧)
Chin. Phys. B, 2020, 29 (**9**): 098102. DOI: 10.1088/1674-1056/abab80

Thermal conductivity characterization of ultra-thin silicon film using the ultra-fast transient hot strip method

Yan-Yan Zhang(张燕燕), Ran Cheng(程然), Dong Ni(倪东), Ming Tian(田明), Ji-Wu Lu(卢继武), Yi Zhao(赵毅)
Chin. Phys. B, 2019, 28 (**7**): 078105. DOI: 10.1088/1674-1056/28/7/078105

Modulated thermal transport for flexural and in-plane phonons in double-stub graphene nanoribbons

Chang-Ning Pan(潘长宁), Meng-Qiu Long(龙孟秋), Jun He(何军)
Chin. Phys. B, 2018, 27 (**8**): 088101. DOI: 10.1088/1674-1056/27/8/088101

SPECIAL TOPIC — Organic and hybrid thermoelectrics

Thermoelectric characteristics of flexible reduced graphene oxide/silver selenide nanowire composites prepared by a facile vacuum filtration process

Zuo Xiao(肖佐), Yong Du(杜永)†, Qiufeng Meng(孟秋风)‡, and Lei Wang(王磊)

School of Materials Science and Engineering, Shanghai Institute of Technology, Shanghai 201418, *China*

(Received 11 October 2021; revised manuscript received 1 December 2021; accepted manuscript online 18 December 2021)

The reduced graphene oxide/silver selenide nanowire (rGO/Ag_2Se NW) composite powders were fabricated via a wet chemical approach, and then flexible rGO/Ag_2Se NW composite film was prepared by a facile vacuum filtration method combined with cold-pressing treatment. A highest power factor of 228.88 $\mu W \cdot m^{-1} \cdot K^{-2}$ was obtained at 331 K for the cold-pressed rGO/Ag_2Se NW composite film with 0.01 wt% rGO. The rGO/Ag_2Se NW composite film revealed superior flexibility as the power factor retained 94.62% after bending for 500 times with a bending radius of 4 mm, which might be due to the interwoven network structures of Ag_2Se NWs and pliability of rGO as well as nylon membrane. These results demonstrated that the GO/Ag_2Se NW composite film has a potential for preparation of flexible thermoelectric devices.

Keywords: thermoelectric, silver selenide, reduced graphene oxide, flexibility

PACS: 81.07.Gf, 81.05.ue **DOI:** 10.1088/1674-1056/ac447e

1. Introduction

Thermoelectric (TE) generators can be used to convert thermal energy into electric energy and have great potentials to meet the future energy demands, due to their advantages of safety, high reliability, small size, no pollution, etc.[1,2] Generally, the energy conversion efficiencies of TE generators are related to TE properties of materials. For a material, its TE properties are limited by the unitless figure-of-merit at their application temperatures ($ZT = \sigma S^2 T/\kappa$), where S, σ, κ and T are the Seebeck coefficient, electrical conductivity, thermal conductivity and temperature in Kelvin, respectively.[3] The σS^2 is called as the power factor (PF), which is often used to evaluate the TE properties of polymer-based materials.[4] TE materials mainly include conducting polymers, inorganic materials and organic-inorganic composite materials.[5–7] Although great advances have been made, it is still a big challenge to acquire a high ZT value since the PF and κ should be carefully optimized.[8–10]

For the purpose of sufficing the needs of newly emerging technologies (i.e., wearable electronics), flexible TE material has been a hot topic due to its distinct features of lightweight, fine pliability and good wearability.[11] More and more researchers have focused their attention on improving TE properties of flexible materials near room temperature.[12–15]

Most recently, many literatures have been reported on flexible n-type TE materials in which silver selenide (Ag_2Se) was employed as the active material.[16–19] For instance, Ding *et al.*[16] fabricated Ag_2Se nanowires (NWs) through a wet chemical template method, and then vacuum filtered the Ag_2Se NWs on nylon substrate to prepare flexible Ag_2Se films. After the hot-pressing treatment, a PF of $\sim$ 987.4 $\mu W \cdot m^{-1} \cdot K^{-2}$ was obtained for the Ag_2Se film at 300 K. Lu *et al.*[17] fabricated flexible Ag_2Se/Ag/CuAgSe composite film via a similar approach, and a PF of 1593.9 $\mu W \cdot m^{-1} \cdot K^{-2}$ at 300 K was acquired. Park *et al.*[20] prepared flexible Ag_2Se/polyvinylidene fluoride (PVDF) composite film by a drop casting approach, and the composite film obtained a PF of $\sim$ 180.6 $\mu W \cdot m^{-1} \cdot K^{-2}$ at 400 K.

Carbon materials (such as graphene and single-walled carbon nanotubes) are always used as the fillers for the preparation of TE composites,[21] due to their high electrical conductivity.[22] For example, flexible Bi_2Te_3 NW/graphene composite film was fabricated through a wet chemical method along with a sintering process, and a PF of $\sim$ 480 $\mu W \cdot m^{-1} \cdot K^{-2}$ was acquired for the Bi_2Te_3NW/graphene composite film (the content of graphene was 80 wt%) at room temperature.[23] Liu *et al.*[22] prepared flexible graphene/poly(3,4-ethylenedioxithiophene):poly(styrenesulfonate) (PEDOT:PSS, PP) composite film by a vacuum filtration approach, and a PF of 29.3 $\mu W \cdot m^{-1} \cdot K^{-2}$ was acquired for the composite film with 2 wt% graphene at 380 K. However, as far as we know, few research on fabrication and TE characteristics of flexible reduced graphene oxide (rGO)/Ag_2Se NW composite films has been reported. Herein, rGO/Ag_2Se NW composite powders were synthesized via a wet chem-

†Corresponding author. E-mail: ydu@sit.edu.cn
‡Corresponding author. E-mail: mengqiufeng@sit.edu.cn

© 2022 Chinese Physical Society and IOP Publishing Ltd

ical process, and flexible rGO/Ag_2Se NW composite films were prepared by a vacuum filtration method combined with a cold-pressing treatment. The morphologies, compositions, TE properties, and pliability of the rGO/Ag_2Se NW composite film were investigated.

2. Experiments and methods

2.1. Chemicals and materials

Graphene oxide (GO) flakes were purchased from Nanjing/Jiangsu XFNANO Materials Tech. Co., Ltd. L-ascorbic acid (LAA, $C_6H_8O_6$, 99%), β-cyclodextrin (β-CD, 99%+), selenium dioxide (SeO_2, 99%+), silver nitrate ($AgNO_3$, 99%), absolute ethanol (AR, 99.5%+), and ethylene glycol (EG, AR, 99.7%+) were provided by Shanghai Titanchem Co., Ltd. Nylon membrane (0.22 μm) was obtained from Millipore Co., Ltd.

2.2. Fabrication of rGO/Ag_2Se NW composites

Firstly, rGO/Se NW composites were synthesized by a wet chemical method. Typically, 1 g SeO_2 powders (Se source) and 1 g β-CD powders were successively added into deionized water (200 mL) with stirring for 0.5 h to form solution A. A certain amount of GO powders were added in deionized water with sonicating for 2 h to obtain solution B. Afterwards, the solution B was added in solution A with agitating for 0.5 h (solution C). 4 g LAA powers were dissolved in deionized water (200 mL) with stirring to form a uniform solution D. Then solution C was added dropwise into solution D with continuously agitating for 4 h to synthesize the rGO/amorphous Se nanoparticle (rGO/Se NP) composite powders. After the reaction, the obtained precipitates were centrifuged (4000 rpm for 3 min), and successively washed with deionized water as well as absolute ethanol for 2–3 times. The rGO/Se NP composites were dispersed in an appropriate volume of absolute ethanol with sonication for 0.5 h, followed by staying for 24 h at ambient temperature. Then the precipitates were centrifuged at 4000 rpm for 3 min, and redispersed in an appropriate amount of EG accompanying with sonication for 0.5 h, resulting in a uniform rGO/Se NW composite dispersion.

The Ag source was prepared by adding a certain weight of $AgNO_3$ in deionized water (40 mL) and agitating until the powders were completely dissolved (solution E). Then solution E was added dropwise to the above rGO/Se NW composite dispersion (the nominal molar ratio of Se source to Ag source was 1:2) with vigorously stirring. The mixed suspension was heated up to 40 °C and maintained at the temperature for 2 h with continuously stirring. After naturally cooled down to ambient temperature, the precipitates were centrifuged at 4000 rpm for 3 min, and alternately washed with deionized water and absolute ethanol for 2–3 times to acquire rGO/Ag_2Se NW composite powders. In the composite powders, the content of rGO was 0.01 wt%.

2.3. Preparation of flexible rGO/Ag_2Se NW composite film

To prepared flexible GO/Ag_2Se NW composite film, the rGO/Ag_2Se NW composite powders were dispersed in absolute ethanol with sonication for 0.5 h to form a homogeneous dispersion, and then the flexible rGO/Ag_2Se NW composite film was prepared by a vacuum filtration method on the nylon membrane. The rGO/Ag_2Se NW composite films were dried at 60 °C under vacuum for 12 h. Finally, the obtained samples were undergone a cold-pressing treatment for 2 min at 30 MPa. Figure 1 presents the schematic illustration of preparation and cold-pressing treatment of flexible rGO/Ag_2Se NW composite films.

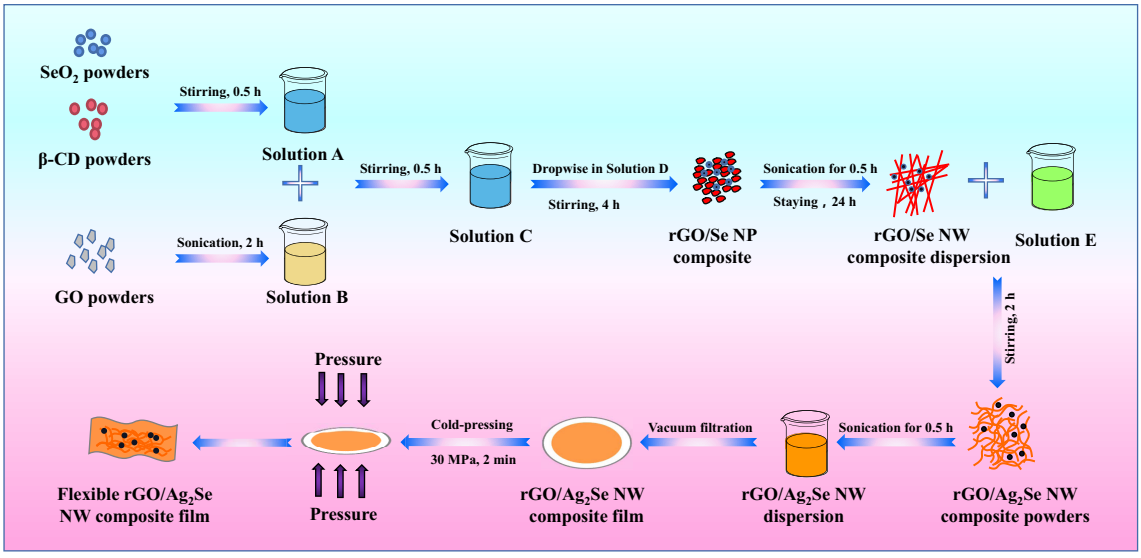


Fig. 1. Illustration of fabrication and cold-pressing treatment of flexible rGO/Ag_2Se NW composite films.

2.4. Measurements and characterizations

The compositions and morphological observations of the rGO/Ag_2Se NW composite film were conducted using x-ray diffraction (XRD, D/max 2200PC, Japan) and field emission scanning electron microscopy (FESEM, Hitachi S-4800, Japan). The thickness of the composite film was determined via the above mentioned FESEM observation. The elemental analysis of the rGO/Ag_2Se NW composite film was carried out via the SEM equipped with an energy dispersive spectrometer (EDS) (FEI Quanta 200 FEG, Netherlands). The measurements of S and σ were carried out by an MRS-3 thin film TE testing facility (Wuhan Giant Instrument Technology Co., Ltd, China) from 297 K to 386 K.

3. Results and discussion

Figures 2(a) and 2(b) are the digital photographs of the pristine and the cold-pressed rGO/Ag_2Se NW composite films on nylon membrane under bending state, respectively. It can be seen that both the composite films show good flexibility, which can be bent and tailored into the desired shapes, and therefore the as-prepared films have the great potentials to be used for the applications of flexible TE devices.

Figure 2(c) is the top-view SEM image of the cold-pressed rGO/Ag_2Se NW composite film. The rGO with flake structure and Ag_2Se NWs with one-dimensional structure can be clearly observed. Moreover, the microstructure of the rGO/Ag_2Se NW composite films is relatively compact, mainly due to the external pressure applied. Figure 2(d) presents the cross-sectional SEM morphology of the rGO/Ag_2Se NW composite film. The average thickness of the rGO/Ag_2Se NW composite film is 5.16 μm. Figure 3(a) shows the selected region of SEM image of the rGO/Ag_2Se NW composite film. The elemental-mapping using the SEM-EDS analysis is displayed in Figs. 3(b)–3(f). The Ag, Se and C elements can be clearly observed in the composite film, where the Ag & Se, and C were attributed to Ag_2Se NWs and rGO, respectively.

Figure 4(a) shows the temperature dependence of the TE performance of the cold-pressed rGO/Ag_2Se NW composite film. The Seebeck coefficient is negative, indicating that the rGO/Ag_2Se NW composite film is an n-type semiconductor. As the temperature increasing from 297 K to 386 K, the absolute value of Seebeck coefficient ($|S|$) tends to first enhance and then minish; at 331 K, the $|S|$ obtains a maximal value of 111.72 $\mu V \cdot K^{-1}$. The change trend of σ is opposite to that of $|S|$, i.e., as the measured temperature rising from 297 K to 331 K, the σ slightly decreases from 188.19 $S \cdot cm^{-1}$ to 183.37 $S \cdot cm^{-1}$. As the temperature further rising to 386 K, the σ enhances to 192.71 $S \cdot cm^{-1}$. As a result, the PF of the cold-pressed rGO/Ag_2Se NW composite film tends to first enhance and then decrease, leading to a highest PF value of 228.88 $\mu W \cdot m^{-1} \cdot K^{-2}$ at 331 K (see Fig. 4(b)). This value is higher than those of the Ag_2Se/PVDF composite film (189.02 $\mu W \cdot m^{-1} \cdot K^{-2}$ at 300 K[24]), the graphene/PP

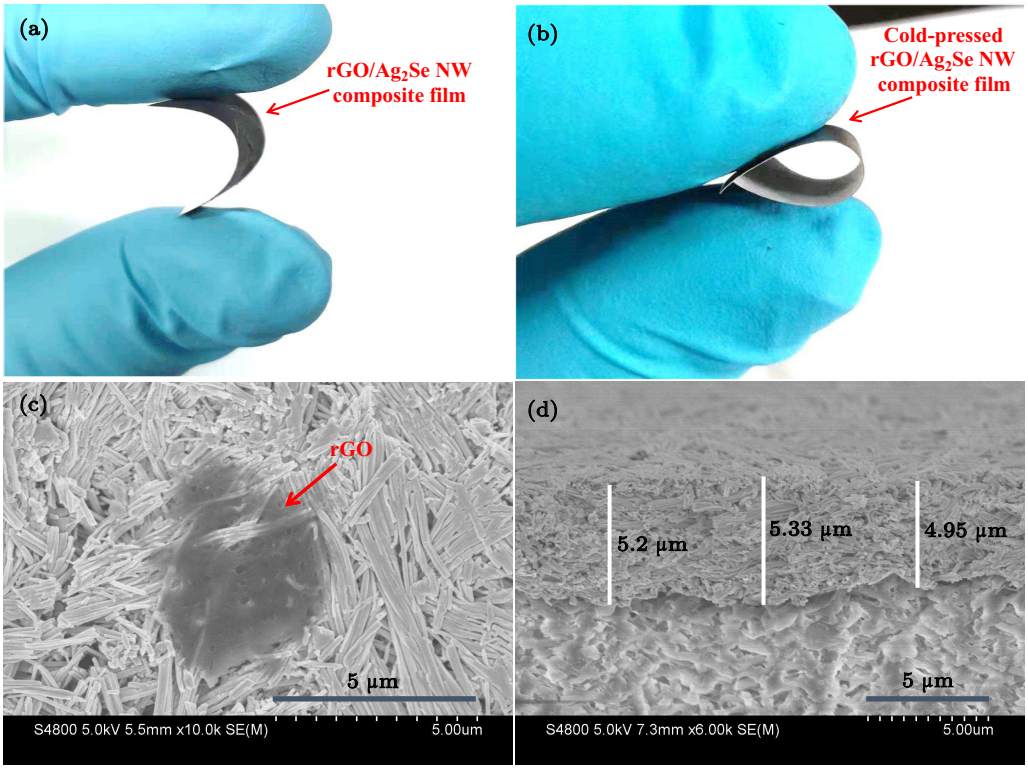


Fig. 2. (a) Digital photo of the rGO/Ag_2Se NW composite film. (b) Digital photo of the cold-pressed rGO/Ag_2Se NW composite film. (c)–(d) SEM images of the cold-pressed rGO/Ag_2Se NW composite film.

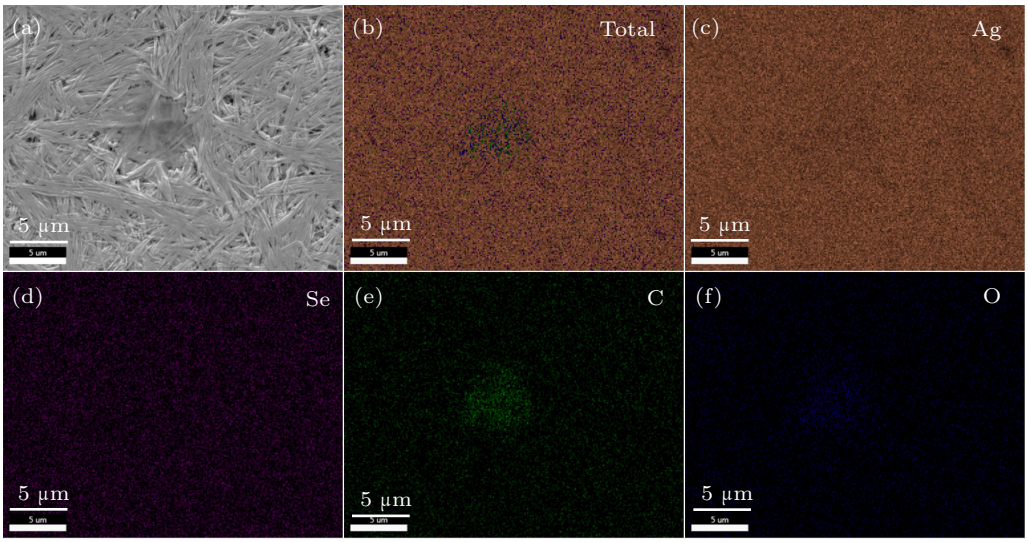


Fig. 3. (a) The selected region of SEM image of cold-pressed rGO/Ag_2Se NW composite film for mapping. SEM-EDS mapping of (b) all element, (c) Ag, (d) Se, (e) C, and (f) O.

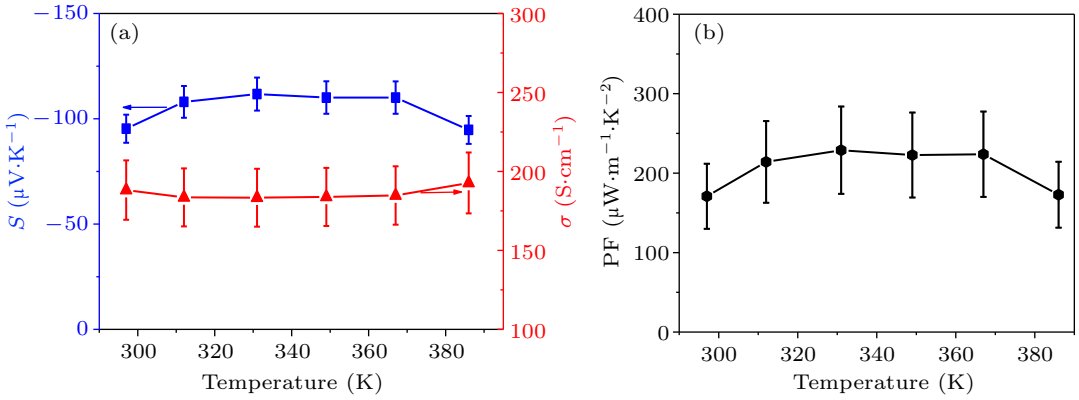


Fig. 4. Temperature dependence of TE properties of cold-pressed rGO/Ag_2Se NW composite film: (a) σ and S; (b) PF.

composite film (29.3 $\mu W \cdot m^{-1} \cdot K^{-2}$ at 380 K),[22] as well as the PP film (224 $\mu W \cdot m^{-1} \cdot K^{-2}$ at room temperature),[15] while lower than those of the Ag_2Se film (1578 $\mu W \cdot m^{-1} \cdot K^{-2}$ at 400 K[25]) and the Ag_2Se/Ag/CuAgSe composite film (1593.9 $\mu W \cdot m^{-1} \cdot K^{-2}$ at 300 K),[17] which might because hot-pressing process was applied in Refs. [17,25]. Table 1 compares TE properties of the cold-pressed rGO/Ag_2Se NW composite film with previously reported flexible TE films.

For investigating pliability, the cold-pressed rGO/Ag_2SeNW composite film was bent with different bending radii and bending times. Figure 5(a) shows the electrical conductivity changes of the composite film after being bent for 100 cycles around diverse bending radii. It is seen that as the radius decreases from 12.5 mm to 4 mm, the retention rate of electrical conductivity only reduces from 98.82% to 96.94%. Figures 5(b) and 5(c) present the TE performance changes of the cold-pressed rGO/Ag_2Se NW composite film as a function of bending cycles when the bending radius is 4 mm. After bending for 500 times, the electrical conductivity reduces to 90%, while the Seebeck coefficient is almost unchanged (Fig. 5(b)). As a result, the PF retains 94.62% after being bent for 500 cycles, demonstrating fine pliability of the rGO/Ag_2Se NW composite film (Fig. 5(c)). The reasons for the good reliability are deduced to be as below: 1) the interwoven networks constructed by the Ag_2Se NWs were formed in the composite film (see Fig. 2(c)); 2) the rGO filler and nylon substrate had good flexibility.

Table 1. TE properties of the cold-pressed rGO/Ag_2Se NW composite film and previously reported flexible TE films (some parameters were calculated from the graphs and tables in the references).

Materials	σ (S/cm)	S ($\mu V \cdot K^{-1}$)	PF ($\mu W \cdot m^{-1} \cdot K^{-2}$)	Temperature (K)	Ref.
PP film	1975	33.4	224	room temperature	[15]
Graphene/PP composite film	~ 976.4	~ 17.3	29.3	380	[22]
Ag_2Se/PVDF composite film	205.52	−95.9	189.02	300	[24]
Ag_2Se/Ag/CuAgSe composite film	7699	−45.5	1593.9	300	[17]
Ag_2Se film	~ 1050	~ −122.6	1578	400	[25]
rGO/Ag_2Se NW composite film	183.37	−111.72	228.88	331	this work

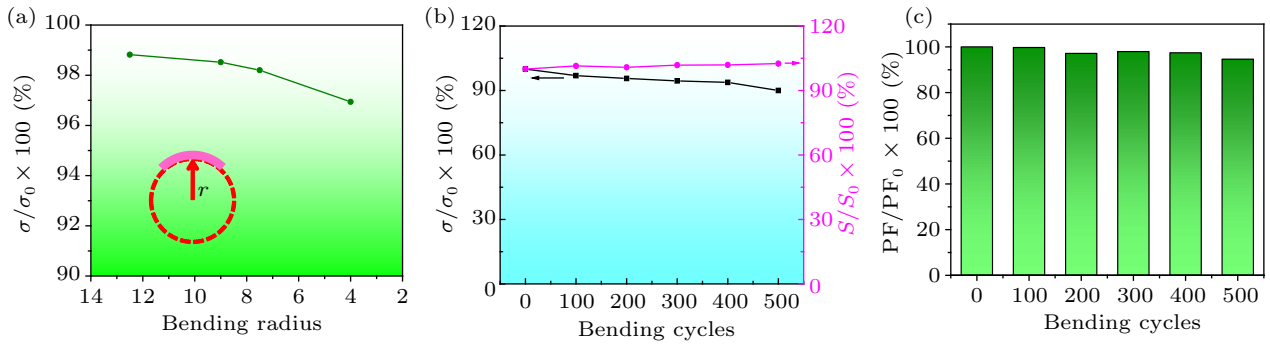


Fig. 5. (a) Electrical conductivity changes of the cold-pressed rGO/Ag_2Se NW composite film vs. diverse bending radii after being bent for 100 cycles. TE performance changes of the cold-pressed rGO/Ag_2Se NW composite film as a function of bending cycles when the bending radius was 4 mm: (b) $|S|$ and σ; (c) PF. The inset in (a) presents the schematic diagram of the bending measurement.

4. Conclusion

In summary, rGO/Ag_2Se NW composite powders were synthesized through a wet chemical method, and flexible rGO/Ag_2Se NW composite films were fabricated through a facile vacuum filtration approach. The cold-pressed rGO/Ag_2Se NW composite film possessed good thermoelectric properties, and a maximum power factor of 228.88 $\mu W \cdot m^{-1} \cdot K^{-2}$ was obtained at 331 K. Moreover, the rGO/Ag_2Se NW composite film presented favorable flexibility as the power factor retained 94.62% after bending for 500 cycles with a radius of 4 mm, due to both the interwoven networks of Ag_2Se NWs and good flexibility of rGO filler as well as the nylon substrate.

Acknowledgements

Project supported by the Program for Professor of Special Appointment at Shanghai Institutions of Higher Learning (Grant No. TP2020068), Shanghai Innovation Action Plan Project (Grant No. 17090503600), and Shanghai Sailing Program (Grant No. 20YF1447300).

References

[1] Zong P A, Zhang P, Yin S J, Huang Y J, Wang Y L and Wan C L 2019 *Adv. Electron. Mater.* **5** 1800842
[2] Lv H C, Liang L R, Zhang Y C, Deng L, Chen Z J, Liu Z X, Wang H F and Chen G M 2021 *Nano Energy* **88** 106260
[3] Du Y, Chen J G, Meng Q F, Dou Y C, Xu J Y and Shen S Z 2020 *Vacuum* **178** 109384
[4] Ou C L, Sangle A L, Datta A, Jing Q S, Busolo T, Chalklen T, Narayan V and Kar-Narayan S 2018 *ACS Appl. Mater. Interfaces* **10** 19580
[5] Du Y, Shen S Z, Cai K F and Casey P S 2012 *Prog. Polym. Sci.* **37** 820
[6] Wei Q S, Mukaida M, Kirihara K and Ishida T 2021 *Thermoelectric Energy Conversion* (Cambridge: Woodhead) pp. 333–345
[7] Cao T Y, Shi X L, Zou J and Chen Z G 2021 *Microstructures* **1** 2021007
[8] Du Y, Xu J Y, Paul B and Eklund P 2018 *Appl. Mater. Today* **12** 366
[9] Zhao L D, Lo S H, Zhang Y S, Sun H, Tan G J, Uher C, Wolverton C, Dravid V P and Kanatzidis M G 2014 *Nature* **508** 373
[10] Xu S D, Shi X L, Dargusch M, Di C, Zou J and Chen Z G 2021 *Prog. Mater. Sci.* **121** 100840
[11] Kim C S, Lee G S, Choi H, Kim Y J, Yang H M, Lim S H, Lee S G, Cho B J 2018 *Appl. Energ.* **214** 131
[12] Liang J S, Wang T, Qiu P F, Yang S Q, Ming C, Chen H Y, Song Q F, Zhao K P, Wei T R, Ren D D, Sun Y Y, Shi X, He J and Chen L D 2019 *Energ. Environ. Sci.* **12** 2983
[13] Meng Q F, Song H J, Du Y, Ding Y F and Cai K F 2021 *J. Materiomics* **7** 302
[14] Jia Y H, Jiang Q L, Sun H D, Liu P P, Hu D H, Pei Y Z, Liu W S, Crispin X, Fabiano S, Ma Y G and Cao Y 2021 *Adv. Mater.* **33** 2102990
[15] Xu S D, Hong M, Shi X L, Li M, Sun Q, Chen Q X, Dargusch M, Zou J and Chen Z G 2020 *Energ. Environ. Sci.* **13** 3480
[16] Ding Y F, Qiu Y, Cai K F, Yao Q, Chen S, Chen L D and He J Q 2019 *Nat. Commun.* **10** 841
[17] Lu Y, Qiu Y, Cai K F, Ding Y F, Wang M D, Jiang C, Yao Q, Huang C J, Chen L D and He J Q 2020 *Energ. Environ. Sci.* **13** 1240
[18] Jiang C, Ding Y F, Cai K F, Tong L, Lu Y, Zhao W Y and Wei P 2020 *ACS Appl. Mater. Interfaces* **12** 9646
[19] Jiang C, Wei P, Ding Y F, Cai K F, Tong L, Gao Q, Lu Y, Zhao W Y and Chen S 2021 *Nano Energy* **80** 105488
[20] Park D, Ju H and Kim J 2021 *J. Ind. Eng. Chem.* **93** 333
[21] Liu W D, Yu Y, Dargusch M, Liu Q F and Chen Z G 2021 *Renew. Sust. Energ. Rev.* **141** 110800
[22] Liu X, Du Y, Meng Q F, Shen S Z and Xu J Y 2019 *J. Mater. Sci.-Mater. El.* **30** 20369
[23] Ju H, Kim M and Kim J 2015 *Chem. Eng. J.* **275** 102
[24] Zhou H J, Zhang Z J, Sun C X, Deng H and Fu Q 2020 *ACS Appl. Mater. Interfaces* **12** 51506
[25] Xu S D, Hong M, Li M, Sun Q, Yin Y, Liu W D, Shi X L, Dargusch M, Zou J and Chen Z G 2021 *Appl. Phys. Rev.* **8** 041404